RSC Sustainability

ROYAL SOCIETY OF CHEMISTRY

PAPER

View Article Online
View Journal | View Issue

Cite this: *RSC Sustainability*, 2025, **3**, 352

Enhanced mechanical strength of polypropylene bionanocomposites through spray-dried nanocrystalline cellulose reinforcement

Fatimah Athiyah Sabaruddin,[a] Hidayah Ariffin, *[ab] Siti Shazra Shazleen,[a] Lawrence Ng Yee Foong,[b] Pim-on Rujitanaroj,[c] Kasinee Thitiwutthisakul,[c] Patcharin Permpaisarnsakul[c] and Phungjai Tinnasulanon[c]

The polymer industry is increasingly focusing on nanocellulose-based polymer composites owing to their remarkable mechanical properties. However, achieving well-dispersed nanocellulose fillers remains challenging. This unique study compares one-step and two-step melt-blending processes for incorporating spray-dried nanocrystalline cellulose (SD-NCC) at 3 and 5 wt% into polypropylene with a 3 wt% MAPP coupling agent. Both the one-step and two-step compounding processes were evaluated for their effects on nanocellulose distribution and mechanical performance. One-step PP/SD-NCC3 achieved the best properties: 34.8 MPa tensile, 57.3 MPa flexural, and 2.08 kJ m^{-2} impact strengths. SEM-EDX confirmed good SD-NCC distribution. Two-step 5 wt% SD-NCC showed slight improvements in mechanical, crystallinity, and thermal properties because of its better dispersion, but the one-step process was sufficient for achieving excellent performance. These findings suggest that spray-dried NCC can streamline compounding for large-scale applications.

Received 11th June 2024
Accepted 25th October 2024

DOI: 10.1039/d4su00295d

rsc.li/rscsus

Sustainability spotlight

Effective manufacturing is crucial today, and the use of powder nanocellulose signifies innovation in sustainable melt-blending processing. Integrating spray-dried nanocrystalline cellulose (SD-NCC) into polypropylene bionanocomposites *via* an efficient compounding process highlights this advancement. Using SD-NCC in powder form aligns with the UN's Sustainable Development Goals (SDGs) for responsible consumption and production (SDG 12), industry innovation (SDG 9), and climate action (SDG 13). This method reduces manufacturing time and energy consumption while ensuring high material performance. The utilization of SD-NCC paves the way for large-scale eco-friendly industrial applications, marking a substantial leap forward in sustainable materials development.

1 Introduction

Sustainable polymer-based composites have attracted remarkable interest for vast applications to meet modern society's demand for suitable high-performance materials and demands from the growing numbers of environmentally conscious consumers, industries, and government. There is a need for alternatives to replace current feedstocks with more sustainable natural materials. Bio-based composites can be developed by reinforcing different types of polymers with various kinds of naturally derived reinforcement, for example, plant fiber, wood fiber, biomass, bio-based carbon, flour, or agricultural waste, to enhance materials' sustainability and help preserve the environment.[1,2]

The use of lignocellulose as a reinforcement material for polymer biocomposites has been preferred for its remarkable performance. Lignocellulosic material comprises three components, *viz.* cellulose, hemicellulose, and lignin. Among these three important components, cellulose has received the most attention from researchers and industrial practitioners for utilization as a reinforcement material. The benefits of cellulose can be further extended when components are isolated into nanoparticles known as nanocellulose.[3] In general, nanocellulose is available in three types: (a) nanocrystalline cellulose or cellulose nanowhiskers (NCC/CNWs), (b) nano-fibrillated cellulose or cellulose nanofibers (NFC/CNFs), and (d) bacterial cellulose (BC). Recent advancements in NCC have significantly propelled the scientific community's interest in the development of nano-scale materials.[4,5] The utilization of nanocellulose presents a promising solution owing to its exceptional mechanical properties, biodegradability, and abundance of

[a]*Department of Bioprocess Technology, Faculty of Biotechnology and Biomolecular Sciences, Universiti Putra Malaysia, Serdang, Selangor, 43400, Malaysia. E-mail: hidayah@upm.edu.my*

[b]*Institute of Tropical Forestry and Forest Products (INTROP), Universiti Putra Malaysia, Serdang, Selangor, 43400, Malaysia*

[c]*Innovation and Product Development Center (IPDC), SCG Packaging Public Company Limited (SCGP), Banpong, Ratchaburi, 70110, Thailand*

various types of advanced applications, including food and healthcare industries.[6] The integration of nanocellulose in polymer composites can lead to the reduction of the reliance on non-renewable resources.[7,8]

The employment of nanocellulose, in particular NCC, as a reinforcing agent in composite systems is most commonly reported in the literature. According to Miao and Hamad, NCC can impart better strength and stiffness to composite systems, along with good corrosion resistance.[9] The utilization of this material could be beneficial by reducing internal stress introduced during the curing process and increasing crosslinking density, thus improving the toughness of the nanocomposite significantly. The superiority and potential of NCC have opened new opportunities for the use of plant-based biomass for innovative industrial applications.[10]

Nevertheless, the manufacturing of nanocellulose-based composites, especially for large-scale production, remains a challenge for academia and industry. Critical factors, including the types and forms of nanocellulose, the polymer used as a matrix, surface modification, and the application of coupling agents, are topics that have frequently been discussed in the literature.[11] Other than that, the processing conditions also play a major role in determining the dispersion properties of nanocellulose in polymer composites.[12,13] In recent studies, nanocellulose-based composites have reportedly been prepared *via* wet compounding through the wet feeding of a nanocellulose aqueous suspension. This method can reduce the degree of aggregation, as the presence of water in the liquid suspension of nanocellulose can act as a lubricant, which reduces the possibility of cellulose degradation during the high thermal process, as well as acts as a transport medium for metering and feeding in the nanocellulose.[14,15] Nonetheless, despite the positive feedback and straightforward processes, the several attempts made to apply wet compounding faced challenges that resulted in composites with inferior properties.[16] It has been reported that the presence of water limits the efficacy of the thermal compounding process.[17] Polymers melt at high temperatures, higher than the boiling point of water. Without a proper venting system, the evaporation of water can contribute to the formation of hydrogen-bonded cellulose agglomerates.[12] Consequently, venting openings are usually positioned at the heating barrels to allow water vapor to escape during the extrusion. The nanocellulose suspension is usually heated before compounding to assist water evaporation.[11] Sudden exposure to nanocellulose at high temperatures, on the other hand, was expected to lead to the self-agglomeration of nanocellulose. Given their strong propensity for hydrogen bonding, subjecting the suspension to an elevated temperature can lead to irreversible agglomeration, thus yielding larger particles that deteriorate the properties of the bio-nanocomposites.[15] In addition, wet compounding is unable to fix the incompatibility properties between hydrophilic nanocellulose with hydrophobic polymers, which still requires the application of a coupling agent, modification, *etc.* Lo Re *et al.*[16] mentioned the infeasibility of this method, resulting from the low content of nanocellulose in the water dispersion, thus leading to inefficient mixing and the agglomeration of nanocellulose, especially for its application on an industrial scale.

As the presence of water leads to detrimental effects during the thermal processing of non-polar thermoplastics, drying the nanocellulose suspension seems necessary for their utilization to prepare polymeric nanocomposites that would be useful for industry.[18] Based on a study done by Peng *et al.*,[19] among all the methods reported so far, the spray-drying technique was proposed as a technically appropriate manufacturing process for drying the nanocellulose as it provides a faster and more efficient process that is also scalable for industrial use.[20,21] It is considered the most cost-efficient technology to produce bulk quantities of dry nanocellulose, particularly NCC, after the purification of the acid as it is much easier to handle, store, and transport.[17,22–24] A similar stand was reported by Blok *et al.*,[25] where drying microfibrillated cellulose (MFC) prevented hornification and thus enhanced the transportation and storage efficiency compared to never-dried MFC. The approach offers more advantages by also reducing the cost associated with handling and storing the materials.

CelluForce NCC™ is one of the examples of the world's largest commercial spray-dried NCCs with 300 tonnes per year[26] production, reflecting the effectiveness of this technique in encouraging a variety of types of products to be developed using bio-based materials such as NCC. The spray-drying technique promotes the formation of particulate NCC, which is beneficial as a nanocomposite reinforcement. Through the drying process, water can be completely removed and needle-like fibrils of NCC are formed into an aggregation of nanoparticles.[22]

Despite the physical properties, the effective utilization of nanocellulose also depends on a homogenous dispersion of the nanofiller in the polymer matrix. Nanocellulose materials are hydrophilic and form strong hydrogen bonding, particularly when in their dry form, which leads to agglomeration.[11] This can be very challenging to overcome, especially when nanocellulose has a high surface area-to-volume ratio, which induces strong interparticle forces that make the agglomeration difficult to break.[27] Thus, compatibilizers or coupling agents are utilized to overcome this problem.[28,29]

Many studies have reported the capability of compatibilizers not only to enhance the interfacial behavior between the polymer matrix and filler but to also be involved in the dispersibility of the filler in the composites.[30–32] Maleic anhydride-grafted polypropylene (MAPP) is one of the common coupling agents used and is commercially available in the form of pellets that are applied during melt compounding. MAPP contains maleic anhydride groups that form covalent bonds with hydroxyl groups on the fillers, creating strong chemical linkages that enhance the stress transfer to the polymer matrix. As a coupling agent, MAPP promotes a better dispersion of fillers and ensures uniform distribution throughout the composites, thus imparting enhanced mechanical performance.[28,29]

In addition, MAPP is also able to act as a nucleating agent, which interacts with nanocellulose additives through esterification or hydrogen bonding, enhancing their dispersion and compatibility. The mechanism has been mentioned by Hwang *et al.*,[33] especially with spray-dried nanocellulose, where the

polypropylene of MAPP integrates with the PP matrix and consequently improves the tensile and flexural properties. Furthermore, MAPP promotes the formation of smaller spherulites and accelerates the crystallization, which reduces the warpage during the process and strengthens the composite materials.

Other than the application of a coupling agent, an improved dispersion of NCC also can be achieved through mechanical processing methods *via* melt-extrusion.[34] In general industrial settings, thermoplastics are melt-mixed with the reinforcement to generate a compound before it is pressed into designated products through compression molding or injection molding to yield composites at a high production rate.[12] It has been found that the particle size and fiber length affect the compounding process, particularly for polymer composites incorporated with nano-scale fibers. This compounding, especially *via* the extrusion process, imparts a major influence affecting the structure of the nanofiller network, especially the distribution and dispersion of the nanocellulose in the polymer composites.[11,34,35] As discussed by Wang *et al.*,[11] dried nanomaterials are bonded together through intermolecular forces. During the melt-mixing process, the agglomerations are subjected to integration forces and extensional forces. Then, as the shear stresses overcome the intermolecular forces of the agglomerates, the nanomaterials are able to de-agglomerate thus leading to a better dispersion in the polymer matrix. Also reported by Krishnamoorti,[36] the melt-extrusion process can provide shear forces that can break up the bundles of agglomerated nanomaterials. Most studies to date, however, have focused on the effect of the screw speed on the extrusion process; for example, the study done by Leszczynska *et al.*,[37] which reported that increasing the screw rotational speed from 50 to 150 rpm improved the distribution of micro-fibrillated cellulose (MFC) in polyamide (PA).

So far, limited studies have been conducted on the effect of multiple extrusion processes on the composites to improve the dispersion process. However, there have been a few discussions on the effect of reprocessing natural-materials-based thermoplastic composites for recycling purposes. Nadali *et al.* reported that sequential processing cycles contributed to polymer matrix chain scission, which resulted from thermal oxidation during the reprocessing of the polymer composites.[38] This led to polymer chain degradation due to the harsh thermal and stress steps employed during the recycling process, thus affecting the performance of the composites, including their mechanical properties. While some studies have reported a reduction of composite performance, some others have underscored improvements of a few mechanical properties in the composites, including enhanced strength and stiffness, attributed to the improved dispersion of the filler within the polymer matrix, higher density, lesser formation of voids, enhanced interfacial properties, and improved hydrophobicity of the composites. These effects, nevertheless, could be attributed to the types of filler used and the number of compounding cycles undergone by the composites.[39–42]

Currently, many industries are focusing on bio-based composites, especially the utilization of nanocellulose due to its exceptional mechanical properties.[43] However, achieving a well-dispersed nanocellulose remains a significant challenge. Therefore, in this study, spray-dried nanocrystalline cellulose (SD-NCC) was applied in the manufacturing of polypropylene-reinforced nanocomposites, and the mechanical performance of the bionanocomposites was evaluated. This study highlights the effect of melt-processing (one-step extrusion and two-step extrusion), which was investigated to demonstrate the feasibility of incorporating SD-NCC, with a focus on how these processing methods influence the performance of the resulting bionanocomposites, especially for large-scale manufacturing, with the aim to reduce the environmental impact associated with traditional composite production.

2 Experimental section

2.1 Materials

The nanocrystalline cellulose suspension (W-NCC) used in this study was provided by SCG Packaging Public Company Limited, Thailand. The W-NCC was produced from high-purity bleached eucalyptus fibers (Alpha cellulose > 95.5%, TAPPI 203) with acid hydrolysis using 5 M hydrochloric acid at 70 °C for 60 min, and subsequently subjected to a mechanical shearing process using a Microfluidizer® Processor M-110P (Microfluidics, USA) for different cycles. After the mechanical process, a suspension of W-NCC with a concentration of 4.5 wt% was obtained. Polypropylene resin and the coupling agent maleic anhydride-grafted polypropylene (MAPP) were purchased from Thai Polyethylene Co., Ltd (Grade: P901J) and Dow Packaging & Specialty Plastics (Grade: FUSABOND™ P613), respectively.

2.2 Spray-drying process for the nanocrystalline cellulose

W-NCC was tested to determine its solid content before the spray-drying process. A total of three readings of moisture content were taken using an A&D MX-50 moisture analyzer (Tokyo, Japan). The known solid concentration of W-NCC was then diluted to 0.1 wt%, and the spray-drying process then took place in a spray dryer (GEA NIRO A/S DK 2860, German). The drying air temperature was 190 °C (inlet) and 107 °C (outlet). The feed flow rate was set at 18 mL min^{-1}.

2.3 Preparation of the PP/SD-NCC bionanocomposites

The polypropylene-reinforced spray-dried nanocrystalline cellulose (PP/SD-NCC) composites, with the addition of the MAPP coupling agent, were compounded at various compositions as listed in Table 1. In this study, the bionanocomposite samples were prepared *via* one-step and two-step compounding processes. The compounding process for one-step compounding was executed using a Labtech 16 mm twin-screw extruder (Bangkok, Thailand) and the process parameters were set as a temperature of 180 °C and screw speed of 45 rpm. The compounded composites were then granulated using a pelletizer obtained from Japan Steel Work (JSW) Ltd (Japan) at a strand speed of 0.2 m min^{-1}. The melt-blending process was repeated for two-step compounding by re-introducing the melt-compounded PP/SD-NCC into the same extruder under the

Table 1 Overall compositions of the PP/SD-NCC bionanocomposites used for the compounding process

Sample	PP	MAPP	NCC
PP	100	—	—
PP/SD-NCC3 (one-step compounding)	94	3	3
PP/SD-NCC3 (two-step compounding)	94	3	3
PP/SD-NCC5 (one-step compounding)	92	3	5
PP/SD-NCC5 (two-step compounding)	92	3	5

same melting conditions as in the first step. All the bionanocomposite samples were then pressed into the designated mold using a hydraulic hot press machine at a temperature of 180 °C and pressure of 110 kg cm^{-2} for 5 min (pre-heat) and 10 min (melting) before analysis. A total of 4 replicates were prepared for each composition. A schematic of the whole process is presented in Fig. 1.

2.4 Characterization of the nanocrystalline cellulose

The size distribution of the SD-NCC was analyzed using a Zetasizer Nano S90 instrument (Malvern Instrument, United Kingdom). About 0.04 wt% SD-NCC was suspended in distilled water and sonicated for 15 min before testing. The crystallinity of the NCCs was determined using a benchtop X-ray diffraction (XRD) system (Rigaku Smartlab, Rigaku Corporation, Tokyo Japan). The crystallinity index (CrI) was calculated based on Segal's method, where I_{200} is the intensity of the highest peak (I_{200}) at 2θ around 22.5°, while I_{am} is the minimum intensity of the amorphous region at 2θ around 18.5°.[44]

$$\text{CrI}\ (\%) = (I_{200} - I_{am})/I_{200} \times 100 \quad (1)$$

The physical dimension of the NCCs was analyzed using a JEOL JEM-2100 transmission electron microscopy instrument (TEM, JEOL Ltd, Tokyo Japan). The NCCs were first diluted in distilled water to obtain a 0.05 wt% suspension and the solution was then sonicated and stained with uranyl acetate prior to imaging.

2.5 Mechanical evaluation of the PP/SD-NCC bionanocomposites

Impact tests were performed based on the Izod Impact Test (Notched) and analyzed using an Instron CEAST 9050 Impact Pendulum system (Instron Corporation, Norwood, MA, USA), which complies with the standard ASTM D256.[45] The impact strength (resilience) was calculated directly by dividing the impact value obtained from the measurement by the thickness of the specimen (dimension J m^{-1}) or by the residual area under the notch (dimension kJ m^{-2}). The standard specimen for ASTM D256 is 64 × 12.7 × 3.2 mm ($2\frac{1}{2} \times \frac{1}{2} \times 1/8$ inch).

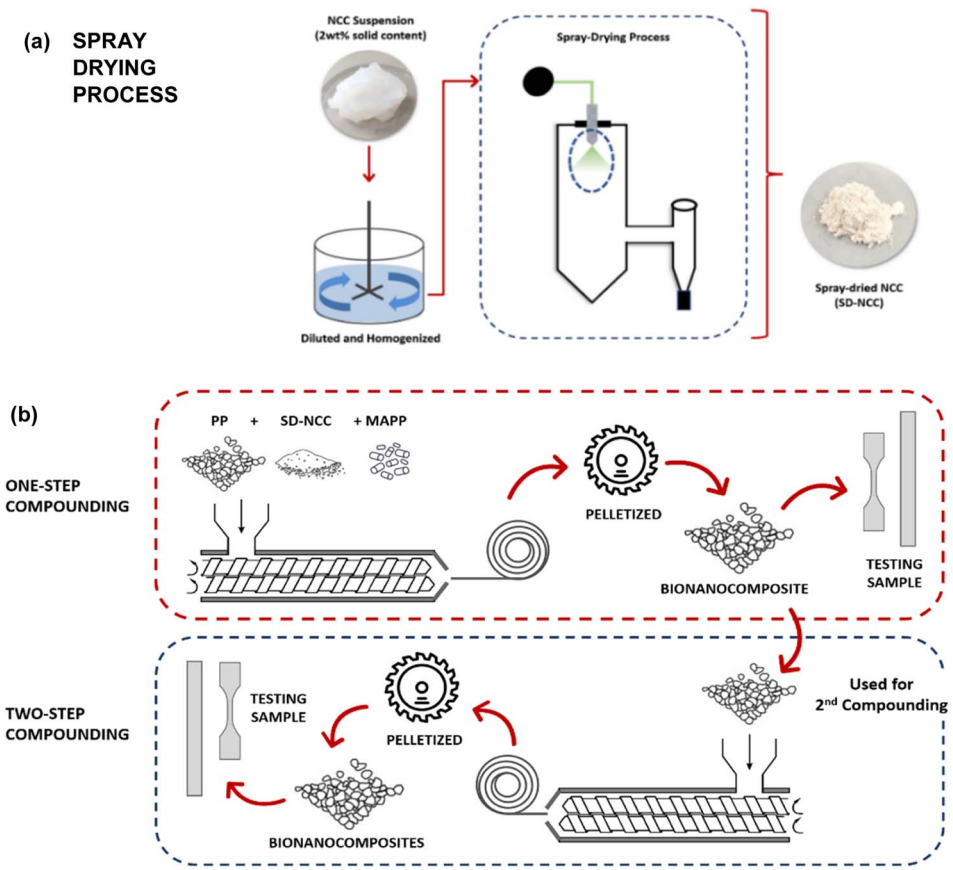

Fig. 1 (a) Spray drying of NCC and (b) one-step and two-step compounding processes.

The tensile properties of the PP/SD-NCC bionanocomposites were analyzed according to the standard ASTM D638.[46] Tensile analysis was evaluated according to ASTM D638 Type 4 Standard, using a universal testing machine (Gotech AI-700L, Gotech Testing Machines Inc., Taiwan) with the aid of extensometer (Epsilon, 3542-025M-100-ST) at a test speed of 5 mm min^{-1}. A total of 4 dog-bone specimens with a thickness of 3 mm were subjected to the tensile tests.

The flexural properties of the PP/SD-NCC bionanocomposites were tested according to the standard ASTM D790,[47] with the sample dimensions of 3.2 mm thick (deep), 12.7 mm wide, and 127 mm long (0.12 × 0.5 × 5 in) using a support span equal to the specimen depth times 16. The test was analyzed using an Instron Universal Testing Machine (Instron 5566, Instron Corporation, Norwood, MA, USA) with a load cell of 30 kN at room temperature. Overall, 4 rectangular specimens were subjected to the test. The speed and span length were determined based on the average dimensions of samples, which were 1.137 mm min^{-1} and 46 mm, respectively.

2.6 Crystallinity index of the PP/SD-NCC bionanocomposites

The crystallinity index properties of the PP/SD-NCC bionanocomposites were determined using a benchtop X-ray diffraction (XRD) system (Rigaku Smartlab, Rigaku Corporation, Tokyo Japan). The crystallinity index of the samples was calculated based on the deconvolution method. The deconvolution of the X-ray diffraction patterns was performed with ORIGIN software considering the Gaussian function as the shape of the resolved peaks. The crystallinity index of the studied samples was calculated by the following equation.

$$\mathrm{CrI}\ (\%) = (A_c/A_t) \times 100 \quad (2)$$

where A_c represents the area of the crystalline domain and A_t is the area of the total domain (crystalline + non-crystalline), respectively.

2.7 Distribution of SD-NCC in the PP bionanocomposites

The distribution of NCC in the PP bionanocomposites was determined *via* elemental mapping of fractured samples using a JSM-7600F field emission scanning electron microscopy system (FESEM, JEOL Ltd, Tokyo Japan) operated at 10 kV. The distribution and dispersion properties of NCC were represented by the distribution of the oxygen element.

3 Results and discussion

3.1 Properties of spray-dried nanocrystalline cellulose (SD-NCC)

3.1.1 Recovery yield of SD-NCC. The NCC obtained from SCG Packaging was in the form of suspension with a 4.5 wt% solid content. A total of 7.5 kg of NCC suspension was used in the spray-drying process. The SD-NCC powder was collected from the sample chamber and weighed to quantify the amount of SD-NCC obtained. Table 2 summarizes the data collected from the spray-drying process. The overall recovery yield of SD-NCC powder was recorded as 56.3%.

Table 2 Recovery yield of SD-NCC after the spray-drying process

Initial weight of NCC suspension (wet basis)	7.5 kg
Initial weight of NCC (dry basis, 4.5% solid content)	0.337 kg
Weight of SD-NCC recovered	0.190 kg
Recovery yield (%)	56.3%

Drying the NCCs in the suspension condition was done after the reduction of the liquid's surface tension in de-ionized water. The suspension was first diluted in de-ionized water and homogenized. The suspension feed rate was optimized at 18 mL min^{-1} during the process. The recovery yield of NCC powder from the spray-drying process was 56.3%. This is higher than the previously reported nanocellulose yields prepared *via* spray-drying, which were in the range of 25–51%.[48] Setter and colleagues[49] discussed that three reasons may contribute to the rather low nanocellulose powder yield obtained from the spray-drying process: (i) adhesion of sticky nanocellulose suspension on the drying chamber wall, (ii) less efficient cyclone in the particles collection chamber, and (iii) high viscosity of the feedstock, which tends to cause fiber agglomeration and adhesion to the wall. Sanders *et al.*[50] explained that other than material agglomeration during drying, large particles could also be formed when there is excess water present at the nozzle tip, whereby during the atomization of water in the air, charge accumulation may produce a coronal discharge, which disrupts the jets and ejected larger droplets. The agglomerated materials then tend to adhere to the wall of the drying chamber, thus affecting the recovered yield of the NCC.

3.1.2 Physical and morphological properties of the SD-NCC. The average particle size of the SD-NCC was determined using a dynamic light scattering (DLS) technique. In colloidal suspensions, like the NCC suspension, DLS analyzes the modulation of the intensity of scattered light as a function of time, which is then mathematically linked with the particle size. In this case, the particle size was measured in the form of the hydrodynamic diameter, which includes the length of the SD-

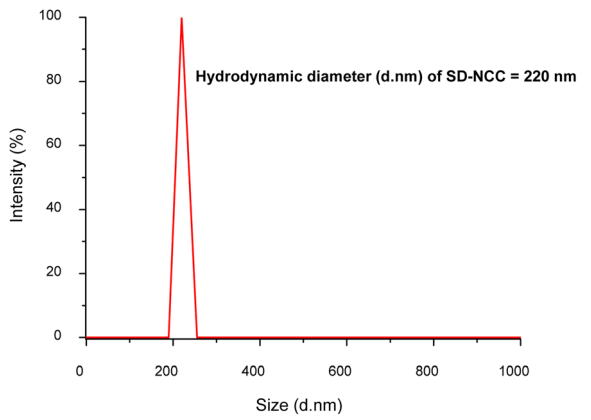

Fig. 2 Particle-size distribution of SD-NCC measured using a DLS analyzer in terms of the hydrodynamic diameter.

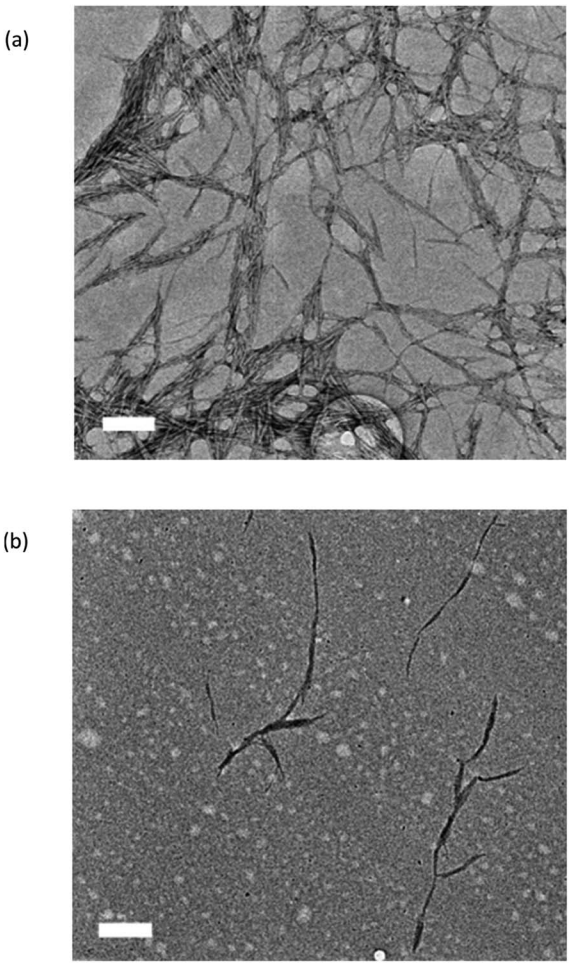

Fig. 3 TEM images of (a) wet NCC (W-NCC) and (b) spray-dried NCC (SD-NCC) at 100 00× magnification.

NCC. Based on the results depicted in Fig. 2, the average particle size of the SD-NCC as analyzed by DLS was determined to be around 200–280 nm.

TEM analysis was conducted to determine the morphology of both the wet and spray-dried NCC (W-NCC and SD-NCC). Both W-NCC and SD-NCC appeared to be in the form of a bunch of needle-like particles with an average width of 10–20 nm and average length of less than a micrometer (Fig. 3). It is common for NCC to have "rod-like" and "needle-like" particles with high crystallinity and a high specific surface area. However, for spray-dried nanocellulose, this was an interesting observation. Even though the SD-NCC was re-dispersed in water prior to the TEM observation, it is understood that generally nanocellulose will form spherical-shaped particles and may agglomerate during spray-drying through atomization of the nanocellulose suspension.[51] Under this condition, it may be difficult to redisperse the NCC completely. Nevertheless, based on Fig. 3b, it was interesting to see that SD-NCC was able to redisperse in water.

To explain this, zeta potential analysis was conducted for the NCC sample, and it was observed that the zeta potential value of the SD-NCC was −25 mV. This indicates that the sample had an almost moderate stability characteristic, which explains the ability of the SD-NCC to redisperse in water.

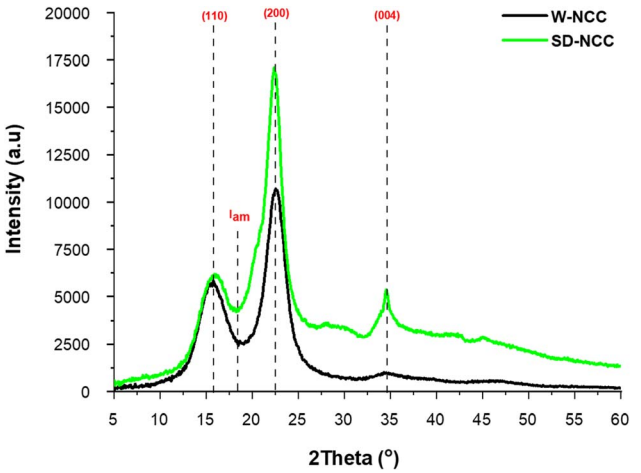

Fig. 4 XRD spectra of W-NCC and SD-NCC.

3.1.3 Crystallinity of W-NCC and SD-NCC. Fig. 4 shows the XRD diffractograms of W-NCC and SD-NCC. The characteristic peaks of NCCs were identified at $2\theta = 15.5°$, 22.3°, and 34.5°, representing the 110, 200, and 004 lattice planes of cellulose I. Both NCCs shared similar peak positions with different intensities. The intensities of the XRD peak can be related to the number of atoms in the crystal, which can affect the X-ray scattering. Meanwhile, other factors also may lead to different peaks, which may depend on the sample condition during the test. Spray-drying typically increases the crystallinity of the NCC, as the removal of water leads to more ordered crystals.[52] In this study, W-NCC was tested in the form of a thin film, while SD-NCC was tested in the form of a pack powder formed on the testing slit. Different forms of the sample tested might lead to peak intensity variations, which occur due to the non-random orientation and large crystallite sizes.[53]

The crystallinity of the NCCs was calculated based on Segal's equation. The crystallinity index (CrI) values of W-NCC and SD-NCC were determined to be 76.2% and 75.0%, respectively. Other studies have reported almost similar crystallinity indices for NCC extracted from bleached eucalyptus.[48] The CrI of NCC could be different when other types of lignocellulose resources are used. For instance, it has been reported that the CrI values of spray-dried NCC extracted from corncob and pine wood were 70.9% and 67.8%, respectively.[54]

3.2 Properties of one-step compounded PP/SD-NCC bionanocomposites

3.2.1 Mechanical properties. Fig. 5 exhibits the mechanical properties of neat PP and PP/SD-NCC bionanocomposites prepared by a one-step compounding process. Both the PP/SD-NCC3 and PP/SD-NCC5 samples were prepared with the addition of 3 wt% MAPP as a compatibilizer. The results showed that the impact strength, tensile modulus, flexural strength, and flexural modulus increased significantly when 3 wt% of SD-NCC was added to the PP. In the case of PP/SD-NCC5, the impact

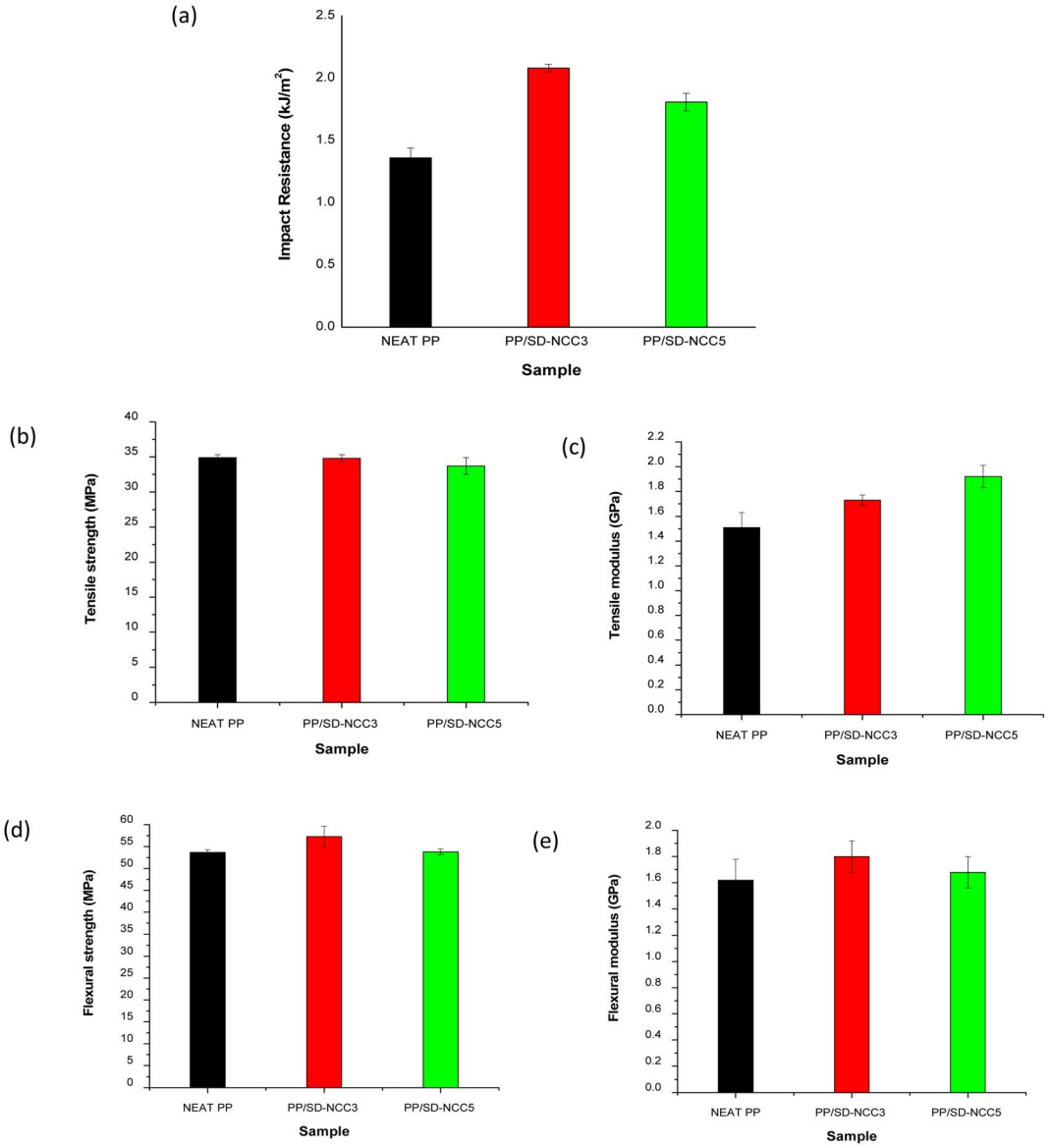

Fig. 5 Profiles of the mechanical properties of polypropylene bionanocomposites at different SD-NCC contents in comparison with neat PP: (a) impact resistance, (b) tensile strength, (c) tensile modulus, (d) flexural strength, and (e) flexural modulus.

strength was 33% higher than that of neat PP; nevertheless, the value was lower than for PP/SD-NCC3. The tensile strength, flexural strength, and flexural modulus values were also lower than those of PP/SD-NCC3 and almost comparable to the neat PP. The tensile strength of neat PP recorded in this study (34.9 MPa) is comparable to those reported in the literature.[55–59] The addition of SD-NCC did not contribute to an increment in the tensile strength value, and in the case of PP/SD-NCC5, the value was lower than that of neat PP. A similar trend was reported by Priyadarsini *et al.*[58]

Above all, it is interesting to note that SD-NCC caused the PP bionanocomposites to be stiffer compared to the neat PP. The higher the SD-NCC composition, the higher the Young's modulus value recorded. Despite showing almost no improvement in tensile strength, SD-NCC seemed to be able to improve the stiffness of the PP. The addition of a nanomaterial is known to be able to improve the stiffness of a polymer, and it is common for a polymer to increase in stiffness with the increase in nanomaterial loading.[60]

SD-NCC was also functional in improving the impact resistance and flexural properties of the PP, as shown in Fig. 5. It has been reported that NCC has a nucleating effect on the polymer matrix to promote the crystallization behavior, resulting in a higher flexural stiffness.[61]

However, after the addition of a higher NCC loading of 5 wt% (PP/SD-NCC5), the flexural strength and modulus were observed to decrease. This might be related to the increment of stiffness of the sample, where the movement of the macromolecular chains of the matrix was hindered.[62] Additionally, at a higher wt% of SD-NCC, some agglomeration may occur, which would cause most of the mechanical properties to be reduced.

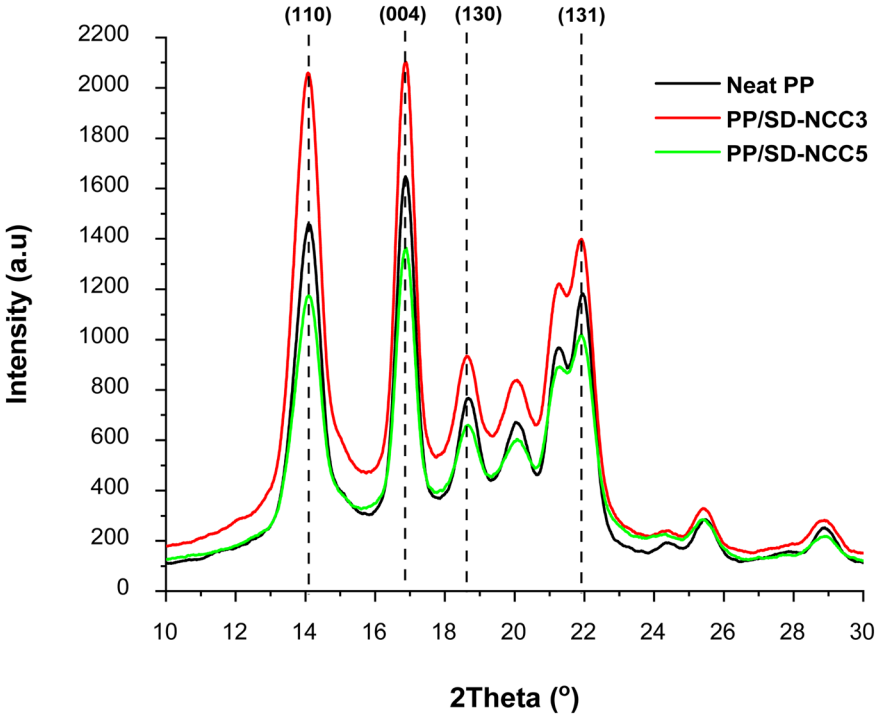

Fig. 6 XRD diffractograms of neat PP and the PP/SD-NCC3 and PP/SD-NCC5 bionanocomposites.

3.2.2 Crystallinity index. The XRD diffractograms of the neat PP, and the PP/SD-NCC-3 and PP/SD-NCC5 bionanocomposites are depicted in Fig. 6. The diffractograms showed apparent peaks referring to PP around 14°, 17°, 18.5°, and 22°. Meanwhile, the crystallinity index (CrI) values for neat PP and the PP bionanocomposites are listed in Table 3. The crystallinity index for neat PP was 52.8%, and this value was found to be in range with the value of polypropylene crystallinity mentioned by Pawlak and Galeski,[63] which was between 30%–60%. As mentioned by Norrrahim *et al.*[64] and Sharip *et al.*,[65] the CrI value of polymer bionanocomposites can be affected *via* the self-nucleation effect (homogenous nucleation) and/or by a nucleation agent (heterogeneous nucleation). The addition of a bio-based filler and coupling agent is known to contribute to heterogeneous nucleation as the fillers may act as nucleating agents and promote crystal growth within the composites, which would consequently increase the crystallinity properties.[33] The addition of SD-NCC on the other hand was shown to reduce the crystallinity index of the bionanocomposites to 46.5% with the addition of 3 wt% of SD-NCC. The decrement was more pronounced with the addition of 5 wt% SD-NCC, leading to a CrI value of 43.3%. Nevertheless, despite the reduction in CrI, the addition of 3 wt% SD-NCC resulted in the highest XRD peak intensities, which was attributed to the enhanced crystalline regions within the PP matrix. This result was also reported by Huang *et al.*,[66] who mentioned that the CrI tendency to decrease could be related to the addition of filler and also the MAPP coupling agent, which acts as a nucleating agent that modifies the crystallization behavior of the PP matrix. Despite the reduction in CrI, the intensities of the peaks in the XRD patterns were found to increase due to the enhanced ordering of the crystalline domains at an optimum concentration of MAPP, which led to more intense diffraction peaks. On the other hand, when the addition of SD-NCC was increased up to 5 wt%, the CrI decreased even more due to disruption of polymer packing, increase in the interfacial interactions, and due to agglomeration.[67,68]

Table 3 Crystallinity index of neat PP and the PP/SD-NCC3 and PP/SD-NCC5 bionanocomposites

Sample	CrI (%)
Neat PP	52.8
PP/SD-NCC3	46.5
PP/SD-NCC5	43.3

3.2.3 Dispersion and distribution of SD-NCC in the PP bionanocomposites. The dispersion and distribution of the NCC in the PP matrix were estimated through FESEM-EDX analysis by analyzing the distribution of the oxygen element in PP/SD-NCC. The FESEM-EDX images of neat PP and PP/SD-NCC are shown in Fig. 7. The oxygen element traces are mapped as green dots in the figure. From the images, the distribution and dispersion of SD-NCC within the polymer matrix could be estimated.

Overall, the EDX images of PP/SD-NCC3 and PP/SD-NCC5 exhibited that the NCC was quite well-distributed, based on the wide distribution of green dots. Nevertheless, in some parts of the images, it could be observed that there were slight agglomerations, especially for PP/SD-NCC5, indicating that some portions of the NCC may not be well-dispersed. This

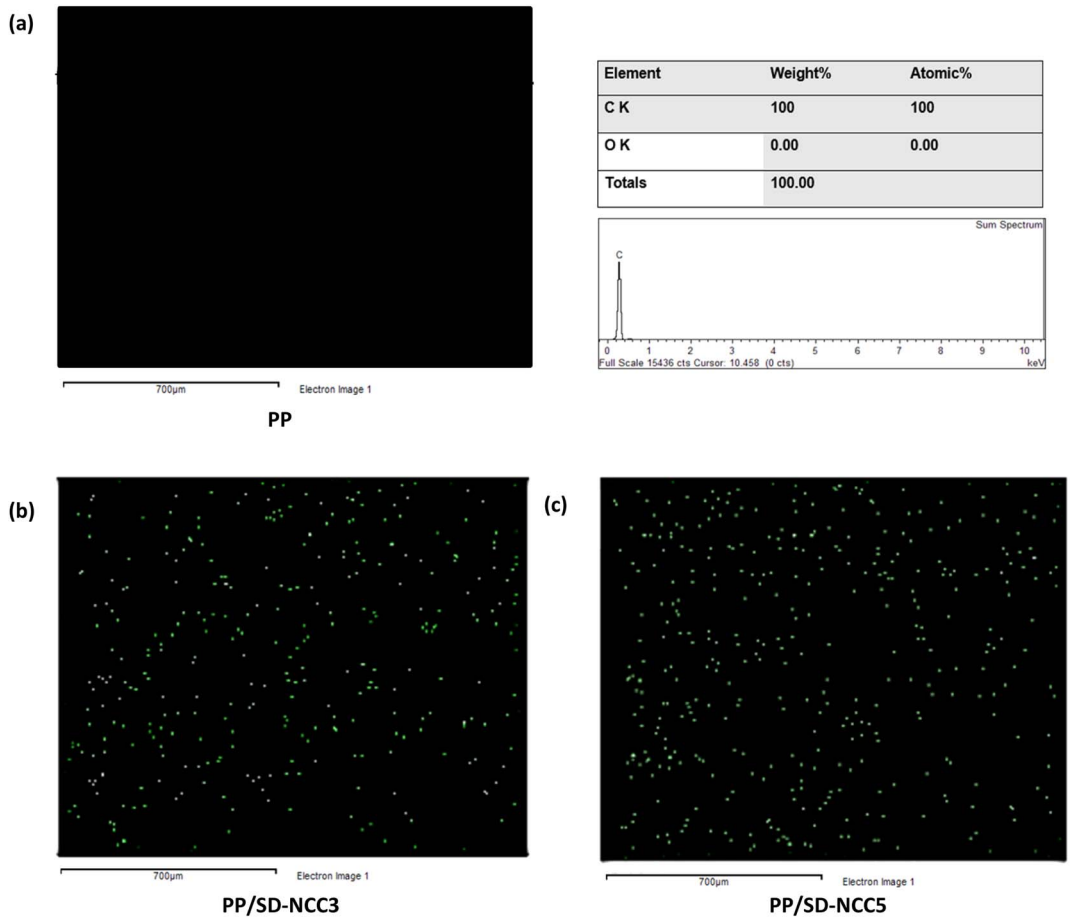

Fig. 7 FESEM-EDX images of (a) neat PP, (b) PP/SD-NCC3, and (c) PP/SD-NCC5. Green dots represent oxygen element distribution in the samples.

observation supports the earlier findings on the tensile strength, flexural strength, and crystallinity, which exhibited slight decrements when 5 wt% of the SD-NCC was used.

3.3. Effect of two-step compounding on the mechanical performance of the PP/SD-NCC3 bionanocomposites

To determine the effect of compounding on the dispersion of the SD-NCC, a two-step compounding process was conducted, and its effect on the mechanical properties of the bionanocomposites was evaluated. For this purpose, the highest addition of NCC in the composites, PP/SD-NCC5 was used.

By focusing on the highest addition of SD-NCC at 5 wt%, the effect of two-step compounding could be analyzed, which could provide insights into the processing–structure–property relationship that is critical for the development of advanced bionanocomposites materials. The results are listed in Table 4. Through the evaluation, it could be seen that there was only a slight improvement in impact resistance, tensile strength, and crystallinity for the PP/SD-NCC5 bionanocomposites with the two-step compounding process. As previously discussed, the increase in NCC loading with the one-step compounding process resulted in a poor dispersion of NCC. While the two-step compounding process was anticipated to enhance NCC dispersion within the PP matrix, as recorded in Table 4, it could be seen that the observed improvements in the respective properties were minimal. These results indicate that although there were some improvements in the distribution of the nanofillers, the overall impact on the load transfer during the

Table 4 Mechanical properties of bionanocomposites prepared *via* the one-step and the two-step compounding process

Sample	Impact resistance (kJ m^{-2})	Tensile strength (MPa)	Tensile modulus (GPa)	Crystallinity (%)
NEAT PP	1.36 ± 0.08	34.9 ± 0.40	1.51 ± 0.12	52.8
PP/SD-NCC5 (one-step)	1.81 ± 0.07	33.7 ± 1.20	1.92 ± 0.10	43.3
PP/SD-NCC5 (two-step)	1.96 ± 0.11	34.1 ± 1.65	1.83 ± 0.11	56.8

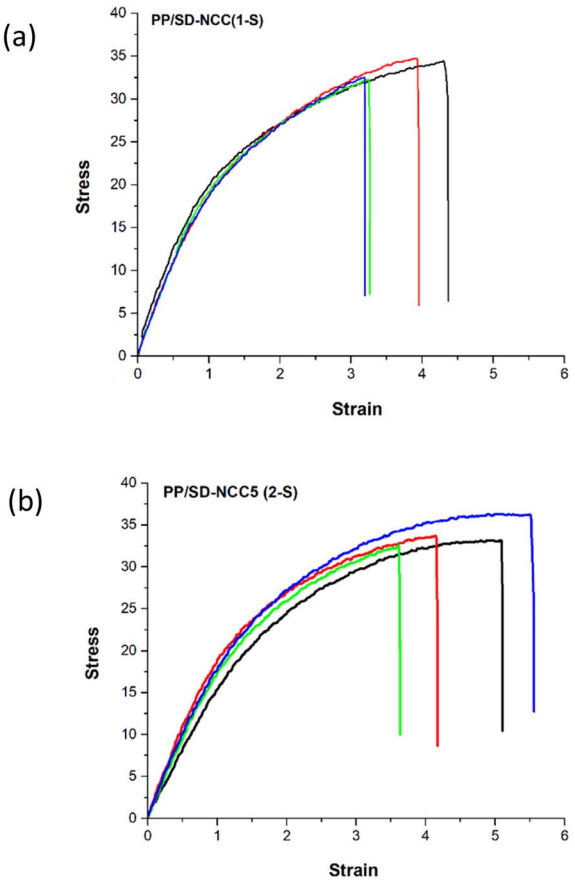

Fig. 8 Stress–Strain curves for PP/SD-NCC5 from (a) one-step and (b) two-step compounding.

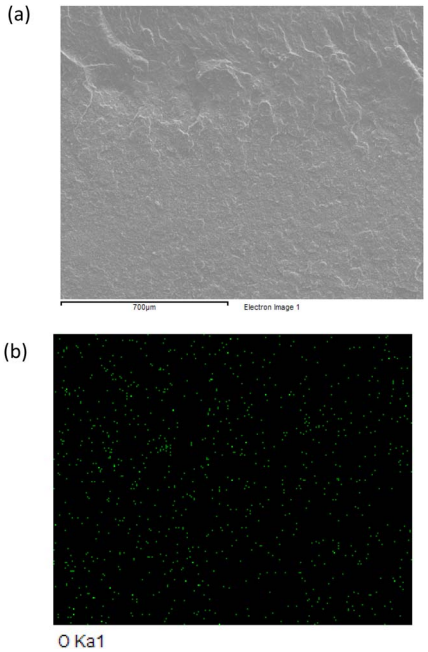

Fig. 9 FESEM-EDX images of PP/SD-NCC5 after two-step compounding (PP/SD-NCC (S-2)).

mechanical stress tests and the subsequent enhancement in the impact resistance and tensile properties of the bionanocomposites were limited.

This finding was supported by the stress–strain curves depicted in Fig. 8. Through this analysis, it could be noted that no pronounced difference in tensile strength between the one-step and two-step processes was observed, with the tensile strength values falling within the one-step process's standard deviation. While the two-step process demonstrated a higher strain capacity, indicating improved ductility, this did not translate into a significant change in tensile strength. These findings suggested that although the processing method can influence specific mechanical properties, such as strain, the overall tensile performance of the composite remained comparable between the two approaches.

The effect of the second compounding process was further evaluated through the FESEM-EDX micrographs presented in Fig. 9. The FESEM micrographs shown in Fig. 9(a) revealed the clear and smooth surface of the PP/SD-NCC5, indicating the improved dispersion of the SD-NCC filler within the polypropylene matrix. Meanwhile, the oxygen mapping conducted using EDX and as illustrated in Fig. 9(b) demonstrated that the SD-NCC filler was distributed more uniformly in the bionanocomposites with 5 wt% SD-NCC content when subjected to the two-step compounding method, indicating an enhanced material homogeneity, in comparison to those produced using a one-step compounding approach, which was attributed to the more refined microstructure. This observation was consistent with the enhancement noted in the mechanical analyses detailed in Table 4, especially for impact strength, where the refinement allowed the materials to absorb more energy before fracturing, thereby increasing the toughness properties of the bionanocomposites. This relationship between the morphology and mechanical properties is consistent with the findings of Saba *et al.*,[69] who indicated that a finer microstructure enhances the ability of materials to withstand impact forces.

Above all, through the mechanical and morphological properties reported earlier, the slight improvement in nanofiller dispersion highlights the complexity of optimizing composite materials, thus suggesting that the processing method can still influence the mechanical performance of the material.

The properties of the bionanocomposites then were reported based on the crystallinity properties. As listed in Table 4, the crystallinity index of the bionanocomposites was found to increase after the two-step compounding process. This result shows the effectiveness of multiple compounding processes in improving the dispersion of filler in the bionanocomposites. The application of shear during the processing could enhance the orientation of the polymer chains, thus improving the crystallization more than that of the bionanocomposites with 3 wt% of SD-NCC. A higher crystallinity indicates stiffer materials, thus imparting higher tensile strength values.

Optical analysis is one of the important evaluations to indicate the effect of nanocellulose addition and distribution in the polymer matrix. The optical properties of the nanocomposites were measured through the intensity of light passing through multiple distribution areas of the composite sample. All the

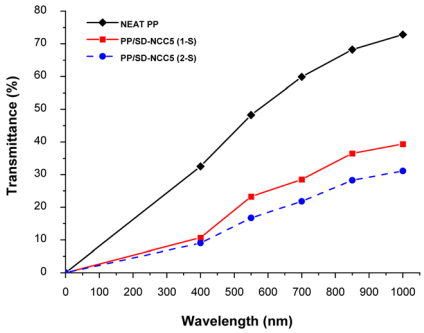

Fig. 10 Optical properties of neat PP and PP/SD-NCC bionanocomposites after one-step and two-step compounding.

samples exhibited different amounts of light passing through them, which was translated through the transmittance spectrum plotted as a function of the visible-light range.

The optical properties of neat PP and PP/SD-NCC bionanocomposites after one-step and two-step compounding are depicted in Fig. 10. In this study, the spectral transmittance of the PP/SD-NCC bionanocomposites film was measured at different wavelengths within the range of 400–1000 nm. All the samples showed an increase in light transmittance up to 1000 nm wavelength. The graph in Fig. 10 shows that the bionanocomposites compounded through a two-step process exhibited lower light transmittance than those compounded

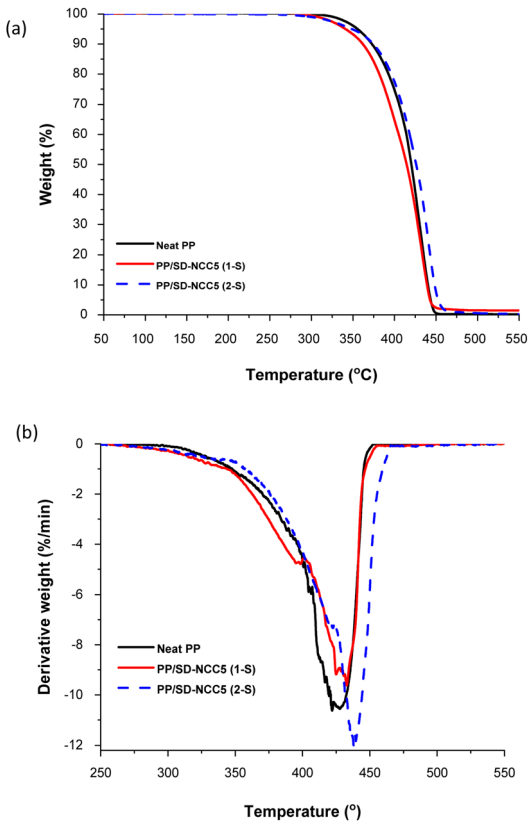

Fig. 11 (a) TGA and (b) DTG thermographs of neat PP and PP/SD-NCC bionanocomposites after one-step and two-step compounding.

Table 5 Thermal stability of neat PP and PP bionanocomposites

Composition	$T_{d50\%}$ (°C)	DTG_{max} (°C)	Char at 500 °C (%)
Neat PP	420.3	427	0.2
PP/SD-NCC5 (one-step)	414.7	432	1.5
PP/SD-NCC5 (two-step)	426.1	438	0.6

through a one-step process. For example, at a wavelength of 700 nm, PP/SD-NCC5 (one-step) had a light transmittance of 30.7% while PP/SD-NCC5 (two-step) showed a lower light transmittance of 21.8%. This phenomenon may be attributed to the more effective distribution of SD-NCC in the bionanocomposite samples achieved through two-step compounding. The repeated compounding may lead to a denser arrangement of SD-NCC particles, thus resulting in increased light scattering and thereby impeding light transmission through the sample.

The thermal analysis results of neat PP and the PP/SD-NCC bionanocomposites compounded through one-step and two-step compounding are depicted in Fig. 11 and listed in detail in Table 5. Based on the data, it was observed that one-step and two-step compounding resulted in different effects, whereby a decrement in $T_{d50\%}$ was seen after one-step compounding, and an increment in $T_{d50\%}$ was observed after two-step compounding. This difference suggested that the compounding process did enhance the thermal stability of the bionanocomposites. Here, the embedded fillers within the polymer matrix can provide better thermal insulation, thus increasing the thermal degradation.[70] These results were also contributed to by the distribution of the SD-NCC in the bionanocomposites, which affected the crystallinity and subsequently their thermal stability. Similar findings have been reported in other studies showing that the thermal stability of polymers can be affected by the crystallinity of the samples.[71,72] This might be due to the addition of nanofillers, such as SD-NCC, which can act as nucleation agents and promote nucleation in the crystallization of the polymer matrix. High-crystallinity polymeric composites then require higher energy for the polymeric chain to be broken down, thus contributing to their better thermal stability properties.[73]

4 Conclusion

Continuous interest has been shown in developing bio-based products to align with sustainability goals and environmental preservation. In this study, spray-dried nanocrystalline cellulose (SD-NCC) served as the main reinforcement to produce polypropylene bionanocomposites through the different stages of the melt-mixing process. Before the compounding stage, the nanocellulose was first subjected to a spray-drying process, and the characterization of both NCCs was discussed, including their dimensional properties, morphologies, and crystallinity properties. The dimensions of the NCC remained in the nanoscale range post spray-drying. The SD-NCC was then employed in the production of bionanocomposites *via* two different mixing conditions: one-step compounding and two-step

compounding. Through the evaluation, the PP/SD-NCC3 bionanocomposites compounded *via* a one-step compounding process showed the optimum mechanical performance with a tensile and flexural strength of 34.8 MPa and 57.3 MPa, respectively, along with the highest impact strength of 2.08 kJ m^{-2}. Elemental mapping *via* EDX revealed an even distribution of oxygen elements, indicating the uniform dispersion of nanocellulose particles. Further evaluation was done for the two-step compounding of PP/SD-NCC5 bionanocomposites. It was found that two-step compounding contributed to the improved mechanical, crystallinity, and thermal properties of the PP/SD-NCC5 bionanocomposites. These findings were attributed to the improved dispersion of SD-NCC when two-step compounding was applied. Overall, the use of spray-dried NCC was found to be feasible, which could contribute to the ease of the compounding process, particularly for large-scale applications. However, marginal improvement was shown for two-step compounding, suggesting that one-step compounding is more suitable for large-scale manufacturing due to its energy efficiency. The one-step compounding can not only achieve sufficient material performance but can also reduce manufacturing time, making it more sustainable for large-scale applications. Moving forward, further study needs to be done to focus on comprehensive feasibility studies to validate the scalability and sustainability of one-step compounding processes for industrial applications.

Data availability

The data for this article have been included as part of the manuscript.

Author contributions

The manuscript was completed through the contributions of all authors. Fatimah Athiyah Sabaruddin: conceptualization, writing – original draft, formal analysis, and data curation. Hidayah Ariffin: conceptualization, writing – review & editing, supervision, project administration, and funding acquisition. Shazra Shazleen and Lawrence Ng Yee Foong: formal analysis and data curation. Kasinee Thitiwutthisakul, Patcharin Permpaisarnsakul, and Phungjai Tinnasulanon: supervision. All authors have read and agreed to the published version of the manuscript.

Conflicts of interest

There are no conflicts to declare.

Acknowledgements

The authors are grateful for the funding provided by SCG Packaging Public Company Limited (SCGP), Thailand to Universiti Putra Malaysia (Grant no. 6380128) for conducting this research

References

1 B. P. Chang, A. K. Mohanty and M. Misra, *RSC Adv.*, 2020, **10**, 17955–17999.
2 Y. Bicer and I. Dincer, *Resour. Conserv. Recycl.*, 2018, **132**, 141–157.
3 D. Trache, A. F. Tarchoun, M. Derradji, T. S. Hamidon, N. Masruchin, N. Brosse and M. H. Hussin, *Front. Chem.*, 2020, **8**, 1–33.
4 T. Abitbol, A. Rivkin, Y. Cao, Y. Nevo, E. Abraham, T. Ben-Shalom, S. Lapidot and O. Shoseyov, *Curr. Opin. Biotechnol.*, 2016, **39**, 76–88.
5 V. Thakur, A. Guleria, S. Kumar, S. Sharma and K. Singh, *Mater. Adv.*, 2021, **2**, 1872–1895.
6 L. P. C. Silva, N. A. de Oliveira, R. S. Valotto, F. C. Monteiro, L. A. C. Alvarez, L. M. Cesário, T. É. C. Zanardo, A. P. M. C. Nilo, R. P. Schuenck, J. P. de Oliveira, F. V. Campos and M. C. C. Guimarães, *Nano-Struct. Nano-Objects*, 2023, **36**, 101045.
7 D. Klemm, F. Kramer, S. Moritz, T. Lindström, M. Ankerfors, D. Gray and A. Dorris, *Angew Chem. Int. Ed. Engl.*, 2011, **50**, 5438–5466.
8 R. J. Moon, A. Martini, J. Nairn, J. Simonsen and J. Youngblood, *Cellulose Nanomaterials Review: Structure, Properties and Nanocomposites*, 2011, vol. 40.
9 C. Miao and W. Y. Hamad, *Curr. Opin. Solid State Mater. Sci.*, 2019, **23**, 100761.
10 A. Dufresne, S. Thomas and L. A. Pothan, *Biopolym. Nanocomposites*, 2013, 1–10.
11 L. Wang, D. J. Gardner, J. Wang, Y. Yang, H. L. Tekinalp, M. Tajvidi, K. Li, X. Zhao, D. J. Neivandt, Y. Han, S. Ozcan, J. Anderson, U. S. F. Service and G. P. Drive, *Composites, Part B*, 2020, **201**, 108297.
12 L. Wang, D. J. Gardner, J. Wang, Y. Yang, H. L. Tekinalp, K. Li, X. Zhao, D. J. Neivandt, Y. Han, S. Ozcan and J. Anderson, *Composites, Part B*, 2020, **201**, 108297.
13 H. Kargarzadeh, M. Mariano, J. Huang, N. Lin, I. Ahmad, A. Dufresne and S. Thomas, *Polymer*, 2017, **132**, 368–393.
14 T. A. T. Yasim-Anuar, H. Ariffin, M. N. F. Norrrahim, M. A. Hassan, Y. Andou, T. Tsukegi and H. Nishida, *Polymers*, 2020, **12**, 1–17.
15 C. Clemons and R. Sabo, *Polymers*, 2021, **13**, 911.
16 G. Lo Re, J. Engström, Q. Wu, E. Malmström, U. W. Gedde, R. T. Olsson and L. Berglund, *ACS Appl. Nano Mater.*, 2018, **1**, 2669–2677.
17 S. Ghasemi, R. Behrooz and M. Rahimi, *Int. J. Nano Dimens.*, 2023, **14**, 167–177.
18 Y. Peng, D. J. Gardner and Y. Han, *Cellulose*, 2012, **19**, 91–102.
19 Y. Peng, Y. Han and D. J. Gardner, *Wood Fiber Sci.*, 2012, **44**, 448–461.
20 S. Sinquefield, P. N. Ciesielski, K. Li, D. J. Gardner and S. Ozcan, *ACS Sustain. Chem. Eng.*, 2020, **8**, 9601–9615.
21 Y. Peng, D. J. Gardner, Y. Han, A. Kiziltas, Z. Cai and M. A. Tshabalala, *Cellulose*, 2013, **20**, 2379–2392.

22 Y. Esparza, T. D. Ngo, C. Fraschini and Y. Boluk, *Ind. Eng. Chem. Res.*, 2019, **58**, 19926–19936.
23 V. Khoshkava and M. R. Kamal, *Powder Technol.*, 2014, **261**, 288–298.
24 D. Burhani, A. A. Septevani, R. Setiawan, L. M. Djannah and A. P. P. Muhammad, *IOP Conf. Ser. Earth Environ. Sci.*, 2022, **1034**, 012033.
25 A. E. Blok, D. P. Bolhuis, K. P. Velikov and M. Stieger, *Food Hydrocolloids*, 2023, **138**, 108398.
26 A. Blanco, M. C. Monte, C. Campano, A. Balea, N. Merayo and C. Negro, *Nanocellulose for Industrial Use: Cellulose Nanofibers (CNF), Cellulose Nanocrystals (CNC), and Bacterial Cellulose (BC)*, Elsevier Inc., 2018.
27 M. Girard, D. Vidal, F. Bertrand, J. R. Tavares and M. C. Heuzey, *Ultrason. Sonochem.*, 2021, **71**, 105378.
28 D.-K. Kim, W. Han, K.-W. Kim and B.-J. Kim, *Polymers*, 2023, **15**, 3784.
29 X. Li, L. Meng, Y. Zhang, Z. Qin, L. Meng, C. Li and M. Liu, *Polymers*, 2022, **14**, 2159.
30 Y. Teramoto, *J. Compos. Sci.*, 2021, **5**, 138.
31 F. A. Sabaruddin, M. T. Paridah, S. M. Sapuan, R. A. Ilyas, S. H. Lee, K. Abdan, N. Mazlan, A. S. M. Roseley and H. P. S. Abdul Khalil, *Polymers*, 2020, **13**, 116.
32 F. A. Sabaruddin, M. Paridah and S. H. Lee, *J. Reinf. Plast. Compos.*, 2019, **38**, 88–95.
33 S. Hwang, Y. Han and D. J. Gardner, *Composites, Part B*, 2024, **268**, 111093.
34 A. M. Kuzmin and E. A. Radaikina, *IOP Conf. Ser.: Mater. Sci. Eng.*, 2020, **873**, 012022.
35 D. Kaczor, K. Bajer, A. Raszkowska-Kaczor, G. Domek, P. Madajski and P. Szroeder, *Materials*, 2022, **15**, 8958.
36 R. Krishnamoorti, *MRS Bull.*, 2007, **32**, 341–347.
37 A. Leszczyńska, P. Kiciliński and K. Pielichowski, *Cellulose*, 2015, **22**, 2551–2569.
38 E. Nadali, M. Layeghi, G. Ebrahimi, R. Naghdi, M. Jonoobi, M. M. Khorasani and Y. Mirbagheri, *Mater. Res.*, 2018, **21**, 1–11.
39 M. D. H. Beg and K. L. Pickering, *Composites, Part A*, 2008, **39**, 1565–1571.
40 M. T. Sarabi, A. H. Behravesh, P. Shahi and E. Soury, *J. Biobased Mater. Bioenergy*, 2012, **6**, 221–229.
41 P. Shahi, A. H. Behravesh, S. Y. Daryabari and M. Lotfi, *Polym. Compos.*, 2012, **33**, 753–763.
42 A. Bourmaud and C. Baley, *Polym. Degrad. Stab.*, 2007, **92**, 1034–1045.
43 A. Dufresne, *Mater. Today*, 2013, **16**, 220–227.
44 L. Segal, J. J. Creely, A. E. Martin and C. M. Conrad, *Text. Res. J.*, 1959, **29**, 786–794.
45 ASTM International, *Annu. Book ASTM Stand.*, 2010, 1–20.
46 ASTM International, 08, *Annu. Book ASTM Stand.*, 2014, 1–16.
47 ASTM International, *Annu. Book ASTM Stand.*, 2010, 1–12.
48 W. T. N. Boschetti, A. M. M. L. Carvalho, A. de, C. O. Carneiro, G. B. Vidaurre, F. J. B. Gomes and D. N. Soratto, *Sustainability*, 2021, **13**, 5888.
49 C. Setter, A. R. P. Mascarenhas, M. C. Dias, A. C. F. de Oliveira Meira, N. T. da Silva Carvalho, M. S. Lorenço, M. A. Martins, G. H. D. Tonoli and T. J. P. de Oliveira, *Ind. Crops Prod.*, 2023, **201**, 116899.
50 J. E. Sanders, L. Wang, G. Brinkley and D. J. Gardner, *Cellulose*, 2023, **30**, 6303–6315.
51 Y. Peng, Y. Han and D. J. Gardner, *Wood Fiber Sci.*, 2012, **44**, 448–461.
52 L. Solhi, V. Guccini, K. Heise, I. Solala, E. Niinivaara, W. Xu, K. Mihhels, M. Kröger, Z. Meng, J. Wohlert, H. Tao, E. D. Cranston and E. Kontturi, *Chem. Rev.*, 2023, **123**, 1925–2015.
53 A. Ali, Y. W. Chiang and R. M. Santos, *Minerals*, 2022, **12**, 205.
54 F. I. Ditzel, E. Prestes, B. M. Carvalho, I. M. Demiate and L. A. Pinheiro, *Carbohydr. Polym.*, 2017, **157**, 1577–1585.
55 B. Alshammari, O. Alothman, A. Alhamidi, M. Jawaid and H. Shaikh, *Materials*, 2022, **15**, 6053.
56 M. N. F. Norrrahim, H. Ariffin, T. A. T. Yasim-Anuar, M. A. Hassan, H. Nishida and T. Tsukegi, *IOP Conf. Ser.: Mater. Sci. Eng.*, 2018, **368**, 1–9.
57 H. M. Hassanabadi, A. Alemdar and D. Rodrigue, *J. Appl. Polym. Sci.*, 2015, **132**, 42438.
58 M. Priyadarsini, T. Biswal and S. K. Acharya, *Mater. Today: Proc.*, 2023, **74**, 980–984.
59 J.-H. Lee, D. H. Kim, Y. Ryu, K. H. Kim, S. H. Jeong, T. Y. Kim and S. W. Cha, *Polymers*, 2021, **13**, 1602.
60 E. C. Demir, M. T. Mcdermott, C. Kim and C. Ayranci, *J. Compos. Mater.*, 2023, **57**, 1087–1104.
61 S. S. Shazleen, L. Y. Foong Ng, N. A. Ibrahim, M. A. Hassan and H. Ariffin, *Polymers*, 2021, **13**, 3226.
62 J. Z. Liang, S. Y. Zou and Q. Du, *Polym. Test.*, 2018, **70**, 434–440.
63 A. Pawlak and A. Galeski, *Crystallization of Polypropylene*, Springer International Publishing, 2019.
64 M. N. F. Norrrahim, H. Ariffin, T. A. T. Yasim-Anuar, M. A. Hassan, N. A. Ibrahim, W. M. Z. W. Yunus and H. Nishida, *Polymers*, 2021, **13**, 1064.
65 N. S. Sharip, H. Ariffin, T. A. T. Yasim-Anuar, Y. Andou, Y. Shirosaki, M. Jawaid, P. M. Tahir and N. A. Ibrahim, *Polymers*, 2021, **13**, 1–15.
66 C.-W. Huang, T.-C. Yang, K.-C. Hung, J.-W. Xu and J.-H. Wu, *Polymers*, 2018, **10**, 382.
67 A. A. B. Omran, A. A. B. A. Mohammed, S. M. Sapuan, R. A. Ilyas, M. R. M. Asyraf, S. S. R. Koloor and M. Petrů, *Polymers*, 2021, **13**, 231.
68 M. Baig, B. Almeshari, A. Aabid, H. Junaedi and A. Almajid, *Heliyon*, 2024, **10**, e30510.
69 N. Saba, P. M. Tahir and M. Jawaid, *Polymers*, 2014, **6**, 2247–2273.
70 A. Jalaee and E. J. Foster, *ACS Sustain. Chem. Eng.*, 2024, **12**, 490–500.
71 N. Samat and M. I. Shafiee, *TEST Eng. Manag.*, 2020, **83**, 25906–25909.
72 A. Chakrabarty and Y. Teramoto, *Polymers*, 2018, **10**, 517.
73 P. G. Gan, S. T. Sam, M. F. bin Abdullah and M. F. Omar, *J. Appl. Polym. Sci.*, 2020, **137**, 48544.